

Crystallographic, optical, and electronic properties of Cu(In,Ga)Se₂ and Cu-deficient phases, Cu(In,Ga)₃Se₅ and Cu(In,Ga)₅Se₈ in Cu₂Se-(In,Ga)₂Se₃ pseudo-binary System

Tsuyoshi Maeda, Kenta Ueda, and Takahiro Wada

Department of Materials Chemistry, Ryukoku University
Seta, Otsu, 520-2194, Japan
Phone: +81-77-543-7468 E-mail: tmaeda@ad.ryukoku.ac.jp

Abstract

We obtained single-phase Cu(In_{1-x}Ga_x)Se₂ (0.0 ≤ x ≤ 1.0) solid solution samples with chalcopyrite-type structure, and Cu(In_{1-x}Ga_x)₃Se₅ (0.0 ≤ x ≤ 0.8) and Cu(In_{1-x}Ga_x)₅Se₈ (0.5 ≤ x ≤ 1.0) samples with stannite-type structure. Their energy levels of the valence band maximum (VBM) were measured by photoemission yield spectroscopy (PYS). The VBM levels of the Cu(In_{1-x}Ga_x)Se₂, Cu(In_{1-x}Ga_x)₃Se₅ and Cu(In_{1-x}Ga_x)₅Se₈ solid solution systems did not change significantly with Ga content, x. The energy levels of the VBM of the Cu(In,Ga)₃Se₅ and Cu(In,Ga)₅Se₈ systems were deeper than that of Cu(In,Ga)Se₂ system. The energy levels of the conduction band minimum (CBM) of the Cu(In_{1-x}Ga_x)Se₂, Cu(In_{1-x}Ga_x)₃Se₅ and Cu(In_{1-x}Ga_x)₅Se₈ systems increased with the Ga content.

1. Introduction

Recently, we reported the crystallographic and optical properties of CuInSe₂, CuIn₃Se₅, and CuIn₅Se₈ phases in the Cu₂Se-In₂Se₃ system [1, 2]. The band-gap energies of Cu-poor Cu-In-Se samples, i.e., CuIn₃Se₅ (1.17 eV) and CuIn₅Se₈ (1.22-1.24 eV), were wider than that of chalcopyrite-type CuInSe₂ (0.99 eV). The valence band maximum (VBM) level of the Cu-poor Cu-In-Se samples significantly decreased with decreasing Cu/In ratio. In order to fabricate high efficiency CIGSe solar cells, we should control the band alignment of CdS/Cu(In,Ga)₃Se₅/Cu(In,Ga)Se₂ interface in the CIGSe solar cells [3]. However, the existence regions, optical properties and electronic structures of Cu(In,Ga)Se₂, Cu(In,Ga)₃Se₅ and Cu(In,Ga)₅Se₈ solid solution systems are still under discussion. The objective of this research is to clarify the crystallographic and optical properties, and band diagrams of Cu-deficient compounds, Cu(In,Ga)₃Se₅ and Cu(In,Ga)₅Se₈ and to compare the obtained results with those of Cu(In,Ga)Se₂.

2. Experimental Procedures

We synthesized Cu(In,Ga)Se₂ and Cu-deficient Cu(In,Ga)₃Se₅ and Cu(In,Ga)₅Se₈ samples (x=0.0, 0.1, 0.2, 0.3, 0.4, 0.5, 0.6, 0.7, 0.8, 0.9, 1.0). Cu(In_{1-x}Ga_x)Se₂, Cu(In_{1-x}Ga_x)₃Se₅ and Cu(In_{1-x}Ga_x)₅Se₈ powder samples with 0.0 ≤ x ≤ 1.0 were prepared by mixing the elemental Cu, In, Ga, and Se powders and sequential heating at 550 °C. The phases in the powders were identified by X-ray powder diffraction (XRD). The band-gap energies of the Cu-poor samples were determined from the diffuse reflectance spectra of the ultraviolet-visible-near infrared spectroscopy.

To understand the band diagram of the ZnO/CdS/CIGSe system, the ionization energies were measured by photoemission yield spectroscopy (PYS). Then, we determined the energy positions of the VBM and CBM of the Cu(In,Ga)Se₂, Cu(In,Ga)₃Se₅ and Cu(In,Ga)₅Se₈ samples from the vacuum level. Then, we discuss band alignment of ZnO/CdS/Cu(In,Ga)Se₂ solar cells with and without insertion of Cu-poor Cu(In,Ga)₃Se₅ layer.

3. Results and discussion

3.1 Crystal phases of (1-y)Cu₂Se-y(In_{1-x}Ga_x)₂Se₃ samples in the Cu₂Se-In₂Se₃-Ga₂Se₃ pseudo-ternary system

The phases in the (1-y)Cu₂Se-y(In_{1-x}Ga_x)₂Se₃ samples in Cu₂Se-In₂Se₃-Ga₂Se₃ pseudo-ternary system were identified by the XRD analysis. In our previous work [1, 2], we reported the crystal structures of CuInSe₂, CuIn₃Se₅, and CuIn₅Se₈ phases in the Cu-poor side of (1-y)Cu₂Se-yIn₂Se₃ (0.5 ≤ y ≤ 1.0) pseudo-binary system. The tie line of the (1-y)Cu₂Se-y(In_{1-x}Ga_x)₂Se₃ samples with x=0.0 and 0.5 < y ≤ 1.0 in Fig. 1 corresponds to our previous reported (1-y)Cu₂Se-yIn₂Se₃ system. As a result, we concluded that the crystal structure of the (1-y)Cu₂Se-yIn₂Se₃ sample changed from a chalcopyrite-type α-phase (y=0.5 and y=0.55) to a stannite-type β-phase (0.60 ≤ y ≤ 0.75) with increasing the content of In₂Se₃, y. The samples with 0.80 ≤ y ≤ 0.95 were a mixed phase of the tetragonal β-phase and hexagonal γ-phase. Our experimental results were in good agreement with the previously reported stable phases in the Cu₂Se-In₂Se₃ pseudo-binary phase diagram [4].

In the reported phase diagram of the Cu₂Se-Ga₂Se₃ system [5], hexagonal γ-phase does not exist, but there is a wide

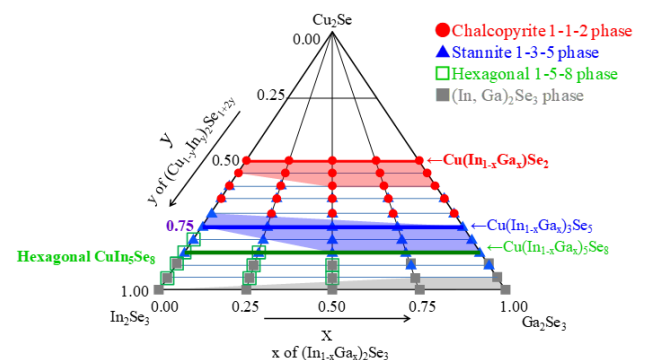


Fig. 1 Schematic crystallographic phases of (1-y)Cu₂Se-y(In_{1-x}Ga_x)₂Se₃ in Cu₂Se-In₂Se₃-Ga₂Se₃ pseudo-ternary system.

region of stannite-type β -phase ($y=0.72-0.86$) in the Cu-poor side of CuGaSe_2 . In present study, the crystal structure of the $(1-y)\text{Cu}_2\text{Se}-y\text{Ga}_2\text{Se}_3$ sample changed from a chalcopyrite-type ($0.50 \leq y \leq 0.60$) to a stannite-type ($0.75 \leq y \leq 0.85$) with increasing the content of Ga_2Se_3 , y . The samples with $0.65 \leq y \leq 0.70$ were a mixture of the tetragonal chalcopyrite-type α -phase and tetragonal stannite-type β -phase. We did not observe a hexagonal γ -phase in the $(1-y)\text{Cu}_2\text{Se}-y\text{Ga}_2\text{Se}_3$ system.

For the $(1-y)\text{Cu}_2\text{Se}-y(\text{In}_{1-x}\text{Ga}_x)_2\text{Se}_3$ samples, we observe that the single-phase region of the chalcopyrite-type $\text{Cu}(\text{In}_{1-x}\text{Ga}_x)\text{Se}_2$ solid solution (α -phase) increases with increasing Ga_2Se_3 content, x . Further, the single-phase region of stannite-type β -phase is also widened by replacement of In by Ga in the $(1-y)\text{Cu}_2\text{Se}-y(\text{In}_{1-x}\text{Ga}_x)_2\text{Se}_3$ samples (with increasing Ga_2Se_3 content, x). Hexagonal γ -phase is not observed in a high Ga_2Se_3 concentration ($x > 0.5$).

3.2 Band gap energies of $\text{Cu}(\text{In}_{1-x}\text{Ga}_x)\text{Se}_2$, $\text{Cu}(\text{In}_{1-x}\text{Ga}_x)_3\text{Se}_5$ and $\text{Cu}(\text{In}_{1-x}\text{Ga}_x)_5\text{Se}_8$ systems

The band-gap energies (E_g s) of the $\text{Cu}(\text{In}_{1-x}\text{Ga}_x)\text{Se}_2$ (a), $\text{Cu}(\text{In}_{1-x}\text{Ga}_x)_3\text{Se}_5$ (b) and $\text{Cu}(\text{In}_{1-x}\text{Ga}_x)_5\text{Se}_8$ (c) samples with $0.0 \leq x \leq 1.0$ were estimated from the $[F(R)/h\nu]^2$ vs. $h\nu$ plot of the reflectance spectra. The E_g of CuInSe_2 ($x = 0.0$) in the tetragonal chalcopyrite phase is 0.99 eV. The E_g of the $\text{Cu}(\text{In}_{1-x}\text{Ga}_x)\text{Se}_2$ solid solution linearly increased from 0.99 eV of CuInSe_2 ($x=0.0$) to 1.65 eV of CuGaSe_2 ($x=1.0$) with increasing Ga content, x .

The E_g of 1.19 eV for CuIn_3Se_5 ($x=0.0, y=0.75$) with the tetragonal stannite structure is larger than that of chalcopyrite-type CuInSe_2 (0.99 eV) ($x=0.0, y=0.50$). The E_g of the $\text{Cu}(\text{In}_{1-x}\text{Ga}_x)_3\text{Se}_5$ solid solution linearly increased from 1.19 eV of CuIn_3Se_5 ($x = 0.0$) to 1.65 eV of CuGa_3Se_5 ($x=1.0$) with increasing Ga content, x . The E_g of the $\text{Cu}(\text{In,Ga})_5\text{Se}_8$ solid solution linearly increases from 1.25 eV of CuIn_5Se_8 ($x=0.0$) to 1.91 eV of CuGa_5Se_8 ($x=1.0$) with increasing Ga content, x .

3.3 Band diagrams of $\text{Cu}(\text{In}_{1-x}\text{Ga}_x)\text{Se}_2$, $\text{Cu}(\text{In}_{1-x}\text{Ga}_x)_3\text{Se}_5$ and $\text{Cu}(\text{In}_{1-x}\text{Ga}_x)_5\text{Se}_8$ systems

Figure 2 (a) shows the band alignment of $\text{ZnO}/\text{CdS}/\text{Cu}(\text{In}_{0.5}\text{Ga}_{0.5})\text{Se}_2$ structure. For CIGSe solar cells, excellent performance can be obtained when the CBM of

window layer is higher by 0-0.4eV (spike-type) than that of CIGSe. Therefore, if a high-Ga $\text{Cu}(\text{In}_{1-x}\text{Ga}_x)\text{Se}_2$ with e.g. $x=0.5$ is applied to an absorber layer of a CIGSe solar cell, the conduction band position of $\text{Cu}(\text{In}_{0.5}\text{Ga}_{0.5})\text{Se}_2$ is higher than that of CdS (-4.1 eV) buffer layer. The conduction band offset at the interface between CIGSe absorber and CdS buffer layers is negative. Unfavorable cliff-type conduction band offset will be formed for higher Ga content of $\text{Cu}(\text{In}_{1-x}\text{Ga}_x)\text{Se}_2$ absorber layer.

Then, we discuss the case of insertion of Cu-deficient layer of stannite-type $\text{Cu}(\text{In}_{0.5}\text{Ga}_{0.5})_3\text{Se}_5$ between $\text{Cu}(\text{In}_{0.5}\text{Ga}_{0.5})\text{Se}_2$ absorber layer and CdS buffer layer in the CIGSe solar cell. Figure 2 (b) shows the band alignment of $\text{ZnO}/\text{CdS}/\text{Cu}(\text{In}_{0.5}\text{Ga}_{0.5})_3\text{Se}_5/\text{Cu}(\text{In}_{0.5}\text{Ga}_{0.5})\text{Se}_2$ structure. As shown in Fig. 2, the band-gap energy of $\text{Cu}(\text{In}_{0.5}\text{Ga}_{0.5})_3\text{Se}_5$ increases, and the VBM becomes deeper compared with the $\text{Cu}(\text{In}_{0.5}\text{Ga}_{0.5})\text{Se}_2$. Therefore, positive valence band offset at the interface between $\text{Cu}(\text{In}_{0.5}\text{Ga}_{0.5})_3\text{Se}_5$ and $\text{Cu}(\text{In}_{0.5}\text{Ga}_{0.5})\text{Se}_2$ layers will be formed. The inserted $\text{Cu}(\text{In}_{0.5}\text{Ga}_{0.5})_3\text{Se}_5$ layer works as a hole blocking layer because the VBM of Cu deficient stannite-type $\text{Cu}(\text{In}_{0.5}\text{Ga}_{0.5})_3\text{Se}_5$ is deeper than that of chalcopyrite-type $\text{Cu}(\text{In}_{0.5}\text{Ga}_{0.5})\text{Se}_2$.

Acknowledgments

This work was partially supported by NEDO under the Ministry of Economy, Trade and Industry (METI).

References

- [1] T. Maeda, W. Gong, and T. Wada, *Jpn. J. Appl. Phys.* **55**, 04ES15 (2016).
- [2] T. Maeda, W. Gong, and T. Wada, *Current Opinion in Green and Sustainable Chemistry* **4**, 77 (2017).
- [3] T. Nishimura, Y. Hirai, Y. Kurokawa, and A. Yamada, *Jpn. J. Appl. Phys.* **54**, 08KC08 (2015).
- [4] N. Kohara, S. Nishiawaki, T. Negami, and T. Wada, *Jpn. J. Appl. Phys.* **39**, 6316 (2000).
- [5] R. Herberholz *et al.*, *Eur. Phys. J. Appl. Phys.* **6**, 131 (1999).

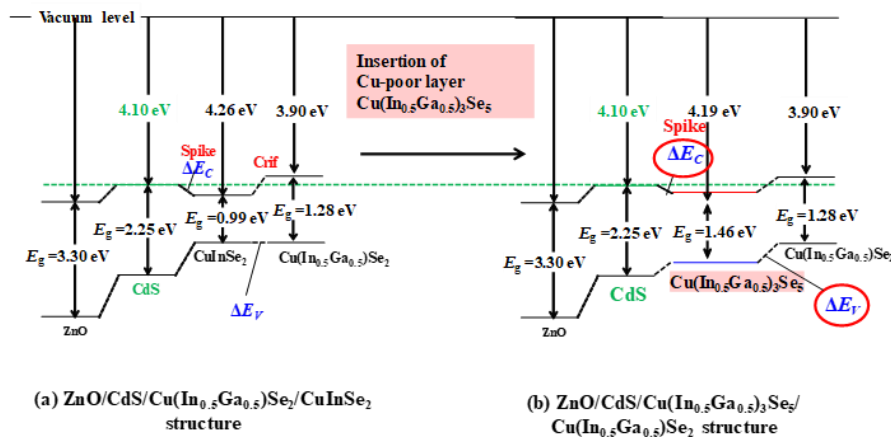


Fig. 2 Band alignment of $\text{ZnO}/\text{CdS}/\text{Cu}(\text{In}_{0.5}\text{Ga}_{0.5})\text{Se}_2$ structure with and without insertion of Cu-poor $\text{Cu}(\text{In}_{0.5}\text{Ga}_{0.5})_3\text{Se}_5$ layer.